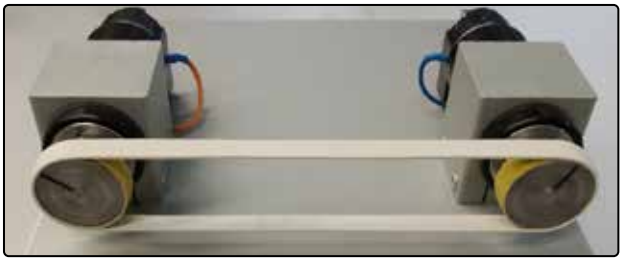

Fig. 3. Illustrative setup with two DC motors and elastic connection.

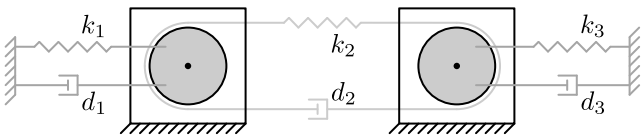

Fig. 4. Schematic drawing of a multivariable setup that consists of two DC motors and an elastic connection.

III. Procedure for Closed-loop Fault Detection Based on Identified Models

In this section, a procedure is presented for the closed-loop fault detection problem described in Section II-B based on identified models from the problem described in Section II-A. This is pursued systematically on the basis of answering the questions i) to iv) proposed in Section II.

A. Standard open-loop identification solution

In this subsection, question i) from Section II is addressed. First, we consider a single-input single-output (SISO) system operating in open loop. The implications of considering a MIMO system and a closed-loop configuration are addressed in III-B.

To obtain an accurate estimate $\widehat{G}_u(e^{j\omega})$ of the system $G_u(e^{j\omega})$, despite the presence of noise, consider one of the various commonly accepted solutions for the open-loop problem. For arbitrary signals u and y, e.g., generated through applying white noise input u, spectral analysis is a commonly applied solution. Here, after averaging over $i = N$ time-frames, the cross-power spectrum of the output and input, $\Phi_{yu}(\omega)$, is divided by the auto-power spectrum of the input, denoted by $\Phi_{uu}(\omega)$. This gives

$$\widehat{G}_u(e^{j\omega}) = \frac{\widehat{\Phi}_{yu}(\omega)}{\widehat{\Phi}_{uu}(\omega)} = \frac{\frac{1}{N}\sum_{i=1}^{N} Y_i(\omega)U_i(\omega)^H}{\frac{1}{N}\sum_{i=1}^{N} U_i(\omega)U_i(\omega)^H}, \quad (9)$$

where H denotes the Hermitian transpose and $Y_i(\omega)$ and $U_i(\omega)$ are the Fourier transforms of y_i and u_i corresponding to the i^{th} frame. For smoothing purposes, typically a window, e.g., a Hamming window, is applied to each frame. Moreover, more frames may be created through overlap. This approach is often referred to as Welch's modified periodogram method [18]. The coherence function can be considered as a quality certificate for the estimate. For estimates of the covariance on the transfer function estimate, the reader is referred to [19]. Despite noise entering the open-loop system, Welch's modified periodogram method provides an accurate solution to minimize the effect of noise so that an accurate FRF estimate is obtained.

B. MIMO and closed-loop implications on model estimate

In this subsection, question i) and ii) from Section II are addressed. Consider the closed-loop configuration from Figure 1, where a SISO system is excited through the signal r. Using the signals u and y, similar to (9) gives the estimate [20, Chapter 10]

$$\widehat{G}_u(e^{j\omega}) = \frac{\widehat{\Phi}_{yu}(\omega)}{\widehat{\Phi}_{uu}(\omega)} = \frac{G_u(e^{j\omega})\Phi_{rr}(\omega) - C^H(e^{j\omega})\Phi_{vv}(\omega)}{\Phi_{rr}(\omega) + |C(e^{j\omega})|^2\,\Phi_{vv}(\omega)}. \quad (10)$$

As a result of the correlation between u and v, a biased estimate is obtained, which may lead to severe consequences for control and fault diagnosis system design. In the worst-case, if the system is solely driven by v, the obtained estimate is equal to the inverse controller.

A method to overcome this bias, is to estimate the FRF indirectly through the sensitivity function S and the process sensitivity function GS. These estimates are given by

$$\widehat{S}(e^{j\omega}) = \frac{\widehat{\Phi}_{ur}(\omega)}{\widehat{\Phi}_{rr}(\omega)} = \frac{\frac{1}{N}\sum_{i=1}^{N} U_i(\omega)R_i(\omega)^H}{\frac{1}{N}\sum_{i=1}^{N} R_i(\omega)R_i(\omega)^H}, \quad (11)$$

and

$$\widehat{G_uS}(e^{j\omega}) = \frac{\widehat{\Phi}_{yr}(\omega)}{\widehat{\Phi}_{rr}(\omega)} = \frac{\frac{1}{N}\sum_{i=1}^{N} Y_i(\omega)R_i(\omega)^H}{\frac{1}{N}\sum_{i=1}^{N} R_i(\omega)R_i(\omega)^H}, \quad (12)$$

respectively. Similarly, to estimate the sensitivity and the process sensitivity, Welch's modified periodogram method may be applied [18]. Then, the estimate of the plant G_u may be obtained through

$$\widehat{G}_u(e^{j\omega}) = \frac{\widehat{G_uS}(e^{j\omega})}{\widehat{S}(e^{j\omega})}. \quad (13)$$

For SISO systems, this provides an accurate estimate.

The approach for open-loop systems through (9) can easily be extended to the MIMO case of the system G_u with k inputs by performing k experiments, where each experiment independently excites one of in the inputs in order to estimate a column of G_u. For alternative approaches, requiring a single experiment, see for instance [12, Chapter 7].

However, for closed-loop systems, the relation (13) has to be handled with care. To illustrate this, consider the MIMO configuration with two inputs and two outputs with a decentralized control configuration, depicted in Figure 5. The relation between input u_1 and output y_1 is now the equivalent plant defined as

$$G^{\text{eq}}_{u,11} := G_{u,11} - \underbrace{\frac{G_{u,12}C_{22}G_{u,21}}{1 + C_{22}G_{u,22}}}_{\text{cross-coupling}}. \quad (14)$$

Similarly,

$$G^{\text{eq}}_{u,22} := G_{u,22} - \underbrace{\frac{G_{u,21}C_{11}G_{u,12}}{1 + C_{11}G_{u,11}}}_{\text{cross-coupling}}, \quad (15)$$

Fig. 5. MIMO closed-loop configuration with decentralized control architecture. The equivalent plants $G^{\text{eq}}_{u,11}$ (■) and $G^{\text{eq}}_{u,22}$ (■) are highlighted.

gives the equivalent plant between input u_2 and output y_2. Clearly, neglecting the interaction due to cross-coupling leads to a biased estimate. In fault diagnosis, working with an equivalent plant has its advantages. For instance, for systems with considerable amount of inputs and outputs, where the engineer is only interested in faults in a specific location or in case not all inputs and outputs are available to the fault diagnosis system.

If an estimate of the true MIMO plant is desired, k independent excitation experiments have to be performed for each input. Each experiment allows to identify a column of the sensitivity estimate $\widehat{S}(e^{j\omega})$ and process sensitivity estimate $\widehat{G_u S}(e^{j\omega})$. Then, the estimate for the true MIMO plant can be obtained through the matrix product

$$\widehat{G}_u(e^{j\omega}) = \widehat{G_u S}(e^{j\omega})\widehat{S}(e^{j\omega})^{-1}. \tag{16}$$

Even though the difference between (13) and (16) is subtle, the obtained estimate may be very different as a result of interaction.

Despite noise entering the closed-loop system during identification, there exist appropriate solutions to minimize its effect. However, the identification solution should carefully be selected such that biases do not enter the estimate on which the fault diagnosis system is designed, i.e., (13) for a SISO plant or the equivalent plants and (16) for the MIMO plant.

C. Open-loop fault detection solution

In this subsection, question iii) from Section II is addressed. To design a linear residual generator Q and minimize the impact of noise on the residual signal, consider the configuration from Figure 2. First, a MIMO system is considered in open-loop configuration. Closed-loop aspects are addressed in Section III-D. The linear residual generator processing the measurable outputs y and known inputs u has input-output relation

$$\varepsilon = Q \begin{bmatrix} y \\ u \end{bmatrix}. \tag{17}$$

Substitution of the open-loop relation for y, i.e., (4) with $C = 0$ and $r = u$ gives

$$\varepsilon = Q \begin{bmatrix} G_u & G_d & G_f \\ I & 0 & 0 \end{bmatrix} \begin{bmatrix} u \\ d \\ f \end{bmatrix}, \tag{18}$$

or equivalently

$$\varepsilon = \underbrace{(Q_u + Q_y G_u)}_{:=G_{\varepsilon u}} u + \underbrace{(Q_y G_f)}_{:=G_{\varepsilon f}} f + \underbrace{(Q_y G_d)}_{:=G_{\varepsilon d}} d. \tag{19}$$

The residual generator Q can always be parameterized such that the residual ε is decoupled from the input u through the design criterion

a) $G_{\varepsilon u} = 0$,

which implies that $Q_u = -Q_y G_u$. The effects of the noise d can usually not be decoupled from ε. Hence, Q_y should be designed to achieve that the residual ε is significantly influenced by all fault entries f_i, where $i = 1, \ldots, q$, and the influence of the noise signal d is negligible. Thus, loosely speaking the two additional design conditions, which have to be fulfilled, are

b) $G_{\varepsilon f} \neq 0$,

c) $G_{\varepsilon d} \approx 0$.

Specifically, the objective is to maximize the gap between the fault detectability and noise attenuation. An optimization-based approach is employed following [9, Chapter 5]. Consider the admissible noise level $\gamma > 0$, imposed through

$$\|G_{\varepsilon d}\|_\infty \leq \gamma, \tag{20}$$

where $\|\cdot\|_\infty$ denotes the $\mathcal{H}_\infty$-norm. For $\gamma > 0$, a normalized value of $\gamma = 1$ can be used via suitable scaling of the residual filter Q. To characterize fault sensitivity, the index

$$\|G_{\varepsilon f}\|_{\infty -} := \min_{1 \leq i \leq q} \|G_{\varepsilon f_i}\|_\infty, \tag{21}$$

is used as a sensitivity measure, covering globally all fault inputs. Other indexes can be used, e.g., based on the least singular values of the frequency-response of $G_{\varepsilon f}$ [21], [22]. Hence, given $\gamma \geq 0$, a stable and proper optimal fault detection filter Q and corresponding optimal fault sensitivity level $\beta > 0$ need to be determined such that

$$\beta = \max_Q \left\{ \|G_{\varepsilon f}\|_{\infty -} \;\middle|\; \|G_{\varepsilon d}\|_\infty \leq \gamma \right\}. \tag{22}$$

The gap $\frac{\beta}{\gamma}$ can be used as measure to assess the quality of the fault detection filter. Through coprime factorization, the poles of the residual generator can be assigned through which the speed of the FD process can be regulated.

In case the residual generator is based on an accurate fit of the non-parametric FRFs obtained through the methods described in Section III-B, the conditions a) to c) are accurately met. Moreover, the effect of noise during residual generation is minimized through the employed optimization-based approach.

D. MIMO and closed-loop implications on fault detection

In this subsection, question iv) from Section II is addressed. As described in Section III-B, closing the control loop has substantial consequences for model estimation. The impact on the fault diagnosis system investigated using closed-loop operators.

Theorem 1 *Let G_u, G_d and G_f be given transfer function matrices for the system described by* (7) *with residual generator* (6)*, shown in Figure 2* (■) *and let G_u, G_d and G_f be the same transfer function matrices for the system described by* (4) *with residual generator* (6)*, shown in Figure 2. Then, decoupling the residual ε from u and maximizing* (22) *for the open-loop configuration leads to the exact same residual generator Q as decoupling the residual ε from r and maximizing* (22) *for the closed-loop configuration. Hence, the residual generation problem is invariant to the feedback-control loop, i.e., invariant to the controller C.*

Hence, the design criteria for the closed-loop configuration are the exact same as a) to c) in the open-loop setting. The proof will be published elsewhere.

This result implies that when the entire MIMO plant G_u is known, the same residual generator can be used in an open-loop as well as in a closed-loop configuration.

In case the equivalent plant is used for fault diagnosis, e.g., because either the full MIMO plant is unknown or since it is of large dimensions, the fault detection problem is *not* invariant to the controller located in the equivalent plant.

Moreover, this result shows that despite the controller attenuating the effect of additive faults, it is equally detectable in the residual, which can be considered as a nice property. Indeed, the residual is thus not a metric that describes the severity of the fault in regard to the performance of the closed-loop system.

IV. Illustrative Case Study

Through this simulation-based case study, the implications of closed-loop feedback on different fault detection filter designs are illustrated. The first filter is designed neglecting the influence of the noise d, the second filter is based on the assumption that interaction may be neglected, and the third filter takes both into account.

Consider the data-generating system described by (8) with $J_1 = J_2 = 0.02$, $k_1 = k_3 = 0.01$, $d_1 = d_3 = 0.02$, $k_2 = 500$ and $d_2 = 0.5$ with transfer function matrix $G_u(s)$ and decentralized controller as depicted in Figure 5, with $C_{11}(s) = \frac{450s+14140}{s}$ and $C_{22}(s) = 1.75s + 110$. Moreover, $G_{d_1}(s) = G_{d_2}(s) = \frac{s}{s+600\pi}$, representing high frequency noise with $d_1, d_2 \sim \mathcal{N}(0, 10^{-2})$.

First, the system dynamics are identified through two independent identical experiments with $r_1, r_2 \sim \mathcal{N}(0, 1)$, of which the result is depicted in Figure 6. The 2×2 MIMO plant is estimated with (16) and the equivalent plants are estimated with (13). Moreover, the bias obtained through estimating with (10) is illustrated through comparison with the true equivalent plants.

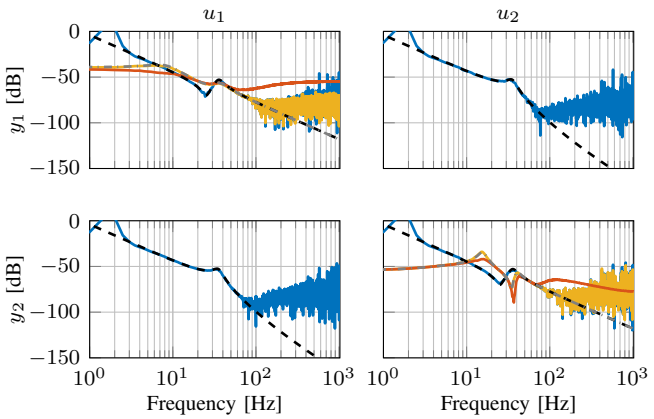

Fig. 6. Estimation of the MIMO transfer function matrix and equivalent plants, compared to the true G_u (- -) and the true equivalent plants $G^{\text{eq}}_{u,11}$ (-·-) and $G^{\text{eq}}_{u,22}$ (-··-). The MIMO estimate $\widehat{G}_u$ (—) is indirectly identified with matrix wise multiplication of the process sensitivity and inverse sensitivity. The equivalent plant estimates $\widehat{G}^{\text{eq}}_{u,11}$ (—) and $\widehat{G}^{\text{eq}}_{u,22}$ (—) are estimated via element-wise division of the process sensitivity and inverse sensitivity. Moreover, the biased estimate (—), identified through the use of solely u and y is depicted.

Assumption 2 *It is assumed that the estimates $\widehat{G}_u$, $\widehat{G}^{\text{eq}}_{u,11}$, $\widehat{G}^{\text{eq}}_{u,22}$ are fit such that the true plants G_u, $G^{\text{eq}}_{u,11}$ and $G^{\text{eq}}_{u,22}$ are obtained for the following fault detection case study.*

The latter is assumed in order to separate the effect of noise during model estimation and during fault detection for a fair comparison of the filter designs. Hence, the effect of biases as a result of model estimation are negated.

Assumption 3 *It is assumed that only the first actuator is sensitive to faults. Hence, it is assumed that only additive faults can enter the system at u_1, shown in Figure 5.*

Since only faults enter the system at u_1, there is no direct interest in the remaining part of the system, i.e., only the equivalent plant $G^{\text{eq}}_{u,11}$ as depicted in Figure 5 is considered. Another motivation to work with this equivalent plant might be that u_2 and y_2 are not directly available for residual generation. Considering $G^{\text{eq}}_{u,11}$, the actuator fault enters y_1 through $G_f = G^{\text{eq}}_{u,11}$. Note that the disturbance d_2 enters y_1 through

$$G^{\text{eq}}_{d_2} := -\frac{G_{u,12}C_{22}}{1 + C_{22}G_{u,22}}G_{d_2}. \tag{23}$$

The first mass is required to follow a sinusoidal setpoint, implemented through the signal $r_1 = C_{11}\bar{r}_1$ with $\bar{r}_1(t) = \sin(0.2\pi t)$. In the remainder, three residual generators are compared on the basis of different assumptions.

(1) Neglecting the influence of noise, i.e., based on $G^{\text{eq}}_{u,11}$, $G_f = G^{\text{eq}}_{u,11}$ and assuming $G_d = 0$.
(2) Neglecting interaction, i.e., based on $G_{u,11}$, $G_f = G_{u,11}$ and G_{d_1}.
(3) Including interaction, i.e., based on $G^{\text{eq}}_{u,11}$, $G_f = G^{\text{eq}}_{u,11}$, G_{d_1} and G^{eq}_{d2}.

The considered additive fault is depicted in Figure 7, as well as the inputs, outputs and reference signal. The normalized residual signals for each of the filter designs are depicted in Figure 8. The residual signal of the first design (—)

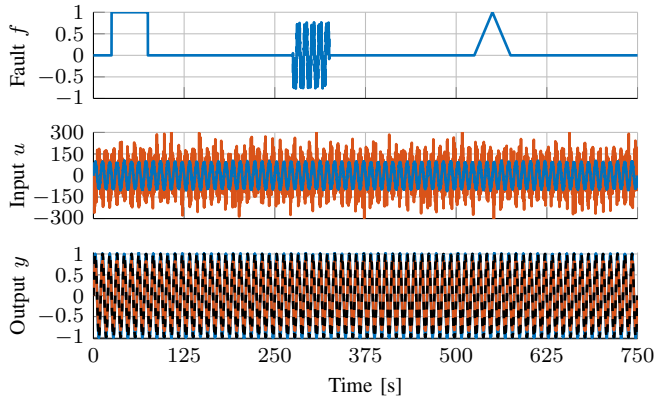

Fig. 7. The actuator fault signal (—), input u_1 (—), input u_2 (—), output y_1 (—), output y_2 (—) and reference $\bar{r}_1$ (- -). Due to closed-loop control, the effect of the fault is attenuated and is not visible in the output.

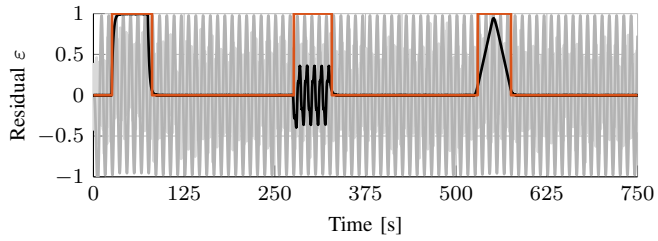

Fig. 8. Comparison of different normalized residual signals, based on the assumptions (1) (—), (2) (—) and (3) (—). A simple fault flag is obtained by taking the absolute value and moving average of the third filter design (—).

performs relatively poorly since noise is neglected, i.e., only the design condition $G_{\varepsilon r}$ is used, leading to the simple residual generator of the form $Q_u = -G^{\text{eq}}_{u,11}$ and $Q_y = 1$. Clearly, the noise is dominating the residual signal, but some effect of the faults can be observed, e.g., most clearly from $25 \leq t \leq 75$.

The second residual generator (—), obtained through the optimization-based approach described in Section III-C performs poorly because the signal r is not decoupled from the residual since $G_{\varepsilon r} \neq 0$. The underlying reason is that the parameterization $Q_u = -Q_y G_{u,11}$ is used, whereas $G^{\text{eq}}_{u,11}$ is the true plant.

The third residual generator (—), obtained through the optimization-based approach described in Section III-C performs well as the interaction is taken into account and the fault to noise ratio is maximized. A simple fault flag (—) is obtained by taking the absolute value of and a moving average of the residual ε.

This illustrative example shows that for this MIMO closed-loop controlled systems, an interpretable residual signal is only obtained through taking the interaction and noise into account for the fault diagnosis system design.

V. Conclusion

The presented identification and fault detection framework in this paper addresses major ambiguities in closed-loop systems. This allows for fault detection in complex systems such as precision mechatronics where only submodules are identified and used in fault diagnosis system. Through an illustrative case study, it is shown that care should be taken with respect to interacting submodules. The presented framework provides a solid basis for fault detection, predictive maintenance and digital twins for complex mechatronic systems.

References

[1] A. Rasheed, O. San, and T. Kvamsdal, "Digital Twin: Values, Challenges and Enablers," pp. 1–31, 2019.

[2] M. Armendia, M. Ghassempouri, E. Ozturk, and F. Peysson, Eds., *Twin-Control: A Digital Twin Approach to Improve Machine Tools Lifecycle*. Springer International Publishing, 2019.

[3] E. C. Balta, D. M. Tilbury, and K. Barton, "A Digital Twin Framework for Performance Monitoring and Anomaly Detection in Fused Deposition Modeling," 2019.

[4] Y. Qamsane, C.-Y. Chen, E. C. Balta, *et al.*, "A Unified Digital Twin Framework for Real-time Monitoring and Evaluation of Smart Manufacturing Systems," 2019.

[5] A. Fuller, Z. Fan, C. Day, and C. Barlow, "Digital Twin: Enabling Technologies, Challenges and Open Research," *IEEE Access*, vol. 8, 2020.

[6] J. Moyne, Y. Qamsane, E. C. Balta, *et al.*, "A Requirements Driven Digital Twin Framework: Specification and Opportunities," *IEEE Access*, vol. 8, 2020.

[7] E. Frisk and M. Nyberg, "A minimal polynomial basis solution to residual generation for fault diagnosis in linear systems," *Automatica*, 2001.

[8] A. Varga, "New computational paradigms in solving fault detection and isolation problems," *Annual Reviews in Control*, vol. 37, no. 1, 2013.

[9] A. Varga, *Solving Fault Diagnosis Problems*. Springer International Publishing, 2017.

[10] T. Oomen, "Advanced Motion Control for Precision Mechatronics: Control, Identification, and Learning of Complex Systems," *IEEJ Journal of Industry Applications*, vol. 7, no. 2, 2018.

[11] L. Ljung, *System Identification - Theory for the User*. Prentice-Hall, 1987.

[12] R. Pintelon and J. Schoukens, *System Identification: A Frequency Domain Approach*, 2nd ed. Hoboken, N.J: John Wiley & Sons Inc, 2012.

[13] P. Van den Hof, "Closed-loop issues in system identification," *Annual Reviews in Control*, vol. 22, 1998.

[14] E. Evers, R. Voorhoeve, and T. Oomen, "On Frequency Response Function Identification for Advanced Motion Control," 2020.

[15] R. Pintelon, P. Guillaume, Y. Rolain, J. Schoukens, and H. Van Hamme, "Parametric identification of transfer functions in the frequency domain-a survey," *IEEE Transactions on Automatic Control*, vol. 39, no. 11, 1994.

[16] R. van Herpen, T. Oomen, and M. Steinbuch, "Optimally conditioned instrumental variable approach for frequency-domain system identification," *Automatica*, vol. 50, no. 9, 2014.

[17] K. Classens, W. P. M. H. Heemels, and T. Oomen, "A Closed-Loop Perspective on Fault Detection for Precision Motion Control: With Application to an Overactuated System," in *2021 IEEE International Conference on Mechatronics (ICM)*, Kashiwa, Japan, 2021.

[18] P. Welch, "The use of fast Fourier transform for the estimation of power spectra: A method based on time averaging over short, modified periodograms," *IEEE Transactions on Audio and Electroacoustics*, vol. 15, no. 2, 1967.

[19] J. Schoukens, G. Vandersteen, Y. Rolain, and R. Pintelon, "Frequency Response Function Measurements Using Concatenated Subrecords With Arbitrary Length," *IEEE Transactions on Instrumentation and Measurement*, vol. 61, no. 10, 2012.

[20] T. Söderström and P. Stoica, *System Identification*. Prentice Hall, 2001.

[21] S. X. Ding, T. Jeinsch, P. M. Frank, and E. L. Ding, "A unified approach to the optimization of fault detection systems," *International Journal of Adaptive Control and Signal Processing*, vol. 14, no. 7, 2000.

[22] I. M. Jaimoukha, Z. Li, and V. Papakos, "A matrix factorization solution to the H-/H∞ fault detection problem," *Automatica*, vol. 42, no. 11, 2006.